

Electronic Structures and Spectra of the Enol Form of Some β -Diketones

Hiroshi MORITA* and Hiroshi NAKANISHI†

The Institute for Solid State Physics, The University of Tokyo, Roppongi, Minato-ku, Tokyo 106

(Received May 29, 1980)

Near and vacuum UV absorption spectra have been measured with benzoylacetone (BA), dibenzoylmethane (DBM), and 3-phenyl-2,4-pentanedione (PPD) in heptane, in acetonitrile, and in ethanol at room temperature. Theoretical analysis of the spectra with the aid of the composite molecule method clearly shows that the π -electron interaction between the enol ring and the benzene ring is rather strong in BA and DBM, but is weak in PPD. The charge-transfer (CT) bands from the benzene ring to the enol ring are observed at 44000 cm⁻¹ in BA, at 40000 and 44000 cm⁻¹ in DBM, and at 41500 and 43800 cm⁻¹ in PPD. The electronic structure of the enol form of malonaldehyde has been elucidated by a modified CNDO-CI method; the result indicates the first and second σ - σ^* excited states predicted at 8.76 and 9.35 eV being the CT band pertinent to the intramolecular hydrogen-bonding.

Keto-enol tautomerism of β -diketones (1,3-propanediones)^{1,2)} has been studied by IR^{3–9)} and NMR^{10–12)} spectroscopies, special attention being paid to solvent and substituent effects on intramolecular hydrogen-bonding (H-bonding) and on chelating ability to a transition-metal atom in forming coordination compounds.^{12–15)} From the IR and NMR studies^{6,10,12)} benzoylacetone (BA), dibenzoylmethane (DBM), 3-phenyl-2,4-pentanedione (PPD), and malonaldehyde (MA) (Fig. 1) are shown to exist predominantly (90–100%) as *cis*-enol form (which has strong intramolecular H-bonding) in pure liquid and in nonpolar solvents.

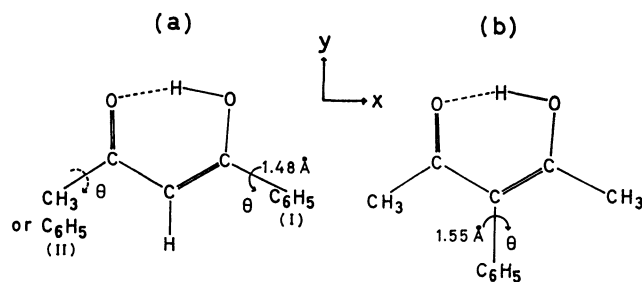


Fig. 1. Molecular structure and parameters for (a) BA and DBM, and (b) PPD. The structure of the enol ring is taken to be the same to the one of MA.

Although the electronic absorption spectra of β -diketones^{16–20)} and of their chelate compounds^{13,17,19,21)} have been measured extensively in the visible and near UV regions, the interpretation of the absorption spectra is rather qualitative. As for the simplest β -diketone, *i.e.*, MA, many theoretical calculations^{22–25)} have been done to investigate molecular geometry and electronic structure in the ground state, special attention being paid to the strong intramolecular H-bonding. Combined with the experimental value of $R(\text{O}\cdots\text{O})=2.55$ Å determined by microwave spectroscopy,²⁶⁾ theoretical results support the molecular geometry of C_s symmetry (asymmetrical H-bond) rather than of C_{2v} symmetry (symmetrical H-bond) in the ground state. Theoretical and experimental investigations of excited states of MA are few.^{27,28)} Excited states of MA are of particular interest in respect to charge-transfer (CT) character

pertinent to H-bond as in the case of acetylacetone (acac) and its fluoro derivatives.^{29,30)} The elucidation of the CT character in the excited states is the first purpose of the present paper.

Phenyl-substituted β -diketones such as BA, DBM, and PPD are expected to have π -electron interaction between the enol ring and the benzene ring.^{6,11,18)} To interpret electronic structure of such large molecules, near and vacuum UV absorption spectra have been measured, and π -electron structure has been investigated by the method of composite molecule.^{31,32)}

Experimental

BA, DBM, and PPD (Tokyo Kasei G. R. grade) were purified by repeated recrystallizations from ethanol and finally by vacuum sublimation. Acetonitrile and heptane (Dotite spectrograde), and ethanol (Wako S. S. grade) were used as solvents without further purification.

Near UV absorption spectra were measured with a Cary recording spectrophotometer model 14, and with a Hitachi recording spectrophotometer model 556, a cell of 1.05 mm light path length being used. Vacuum UV absorption spectra were measured with a spectrophotometer constructed in our laboratory,^{30,33)} a cell of 0.134 mm light path length being used.

Theoretical

The electronic structure of MA was calculated by a modified CNDO-CI method.³⁴⁾ The semiempirical parameters of H, C, and O atoms were taken to be the same as reported previously.^{30,34)} The electronic structures of the π -electron systems for the enol form of BA, DBM, and PPD were calculated by the method of composite molecule^{31,32)} by considering the configuration interaction (CI) among the ground, locally excited (LE), and CT configurations constructed from π -MO's of benzene³²⁾ and MA (corresponding to the enol ring) calculated above. The four LE configurations ($^1B_{2u}$, $^1B_{1u}$, and $^1E_{1u}$) of the benzene ring and the lower two LE configurations (denoted as ψ_1 and ψ_2) of the enol ring were taken into account. The energies of the LE configurations were evaluated from the observed transition energies of benzene (4.86 and 6.08 eV in heptane,³⁵⁾ 6.98 eV in the vapor phase³²⁾, of acac (4.56 and 7.04 eV in perfluorohexane²⁹⁾), and of MA (5.08 eV in ethanol,²⁸⁾ 7.87 eV calculated in the present

† Present address: Toshiba Research and Development Center, 1, Toshiba-cho, Komukai, Saiwai-ku, Kawasaki 210.

paper (Table 4)) combined with the electrostatic interaction energies between excited configuration of the benzene ring and the ground configuration of the enol ring.

Concerning the combination of each of the benzene rings with the enol ring, four CT (from benzene to the enol ring) and four back CT (from the enol ring to benzene) (BCT) configurations were considered. Their energies were evaluated by the usual formula;^{31,32)} $I-A-Q$, where I is the ionization potential of electron donor, A , the electron affinity of electron acceptor, and Q , the electrostatic energy between electron donating and electron accepting MO's including electrostatic interaction energy between the ground configuration of the enol ring and the vacant MO's of the benzene ring. Ionization potentials were taken from the study by photoelectron spectroscopy of benzene,³⁶⁾ acac,^{37,38)} and MA.³⁸⁾ The electron affinity was taken to be -1.0 eV for the benzene ring,³²⁾ and assumed for the lower two vacant π -orbitals of the enol ring to be 0 eV and -2.4 eV in both BA and DBM, and to be 0.5 eV and -1.9 eV in PPD. Two-center Coulomb repulsion integrals necessary for the evaluation of Q were calculated by the use of Klopman's equation.^{34,39)}

The resonance integral, β , in the off-diagonal matrix elements^{31,40)} of the total electronic Hamiltonian was considered only to the C-C bond between the benzene ring and the enol ring by the formula, $\beta = 9.73 \times S$, where S is the overlap integral between the $2p\pi$ AO's of bonded C atoms.

The full matrices (15×15 for BA and PPD, 27×27 for DBM) of the total electronic Hamiltonian were solved to obtain energy levels and wave functions of the whole molecules. Oscillator strength for each absorption band was calculated by taking transition dipole moments between all pairs of the configurations into account. Each transition moment was evaluated including all

the terms up to the first order in overlap, S .

The bond lengths and bond angles of MA were taken from the *ab initio* calculations by Karlström, *et al.*²⁴⁾ and by Del Bene and Kochenour,²⁵⁾ respectively. The O...O distance was taken to be 2.55 Å from the analysis of microwave spectrum,²⁶⁾ and the position of the hydrogen-bonded hydrogen atom, from the X-ray crystal analysis of DBM.⁴¹⁾

In BA, DBM, and PPD, the benzene ring(s)⁴¹⁾ with $r(\text{C-C}) = 1.389$ Å is(are) bonded to the enol ring through the C-C bond(s) of 1.48 Å in BA and DBM,⁴¹⁾ and of 1.55 Å in PPD. The angle, θ , between the planes of the enol ring and the benzene ring was treated as a variable in the actual calculations. As is shown in Fig. 1, BA is enolized toward the phenyl group.⁶⁾

Results and Discussion

Near and Vacuum UV Absorption Spectra of BA, DBM, and PPD. Near and vacuum UV absorption spectra observed with the heptane solutions of BA, DBM, and PPD are shown in Fig. 2. The spectra measured in ethanol and acetonitrile show only a slight shift of the bands, and are essentially the same as the spectra of the corresponding molecules in heptane. The observed band positions and intensities are tabulated in Tables 1–3. As pointed out by the NMR^{10,12)} and IR⁶⁾ spectroscopic studies, the β -diketones under considerations predominantly exist as the *cis*-enol form at room temperature. The spectra shown in Fig. 2 and Tables 1–3 are due to the enol form. Compared to the spectrum of acetylacetone reported previously,²⁹⁾ the first allowed band at ≈ 300 nm shifts to longer wavelengths with increasing intensity in the order of $\text{acac} \leq \text{PPD} < \text{BA} < \text{DBM}$.

Electronic Structure of MA. Preliminary calculations of MA have been done on the basis of different

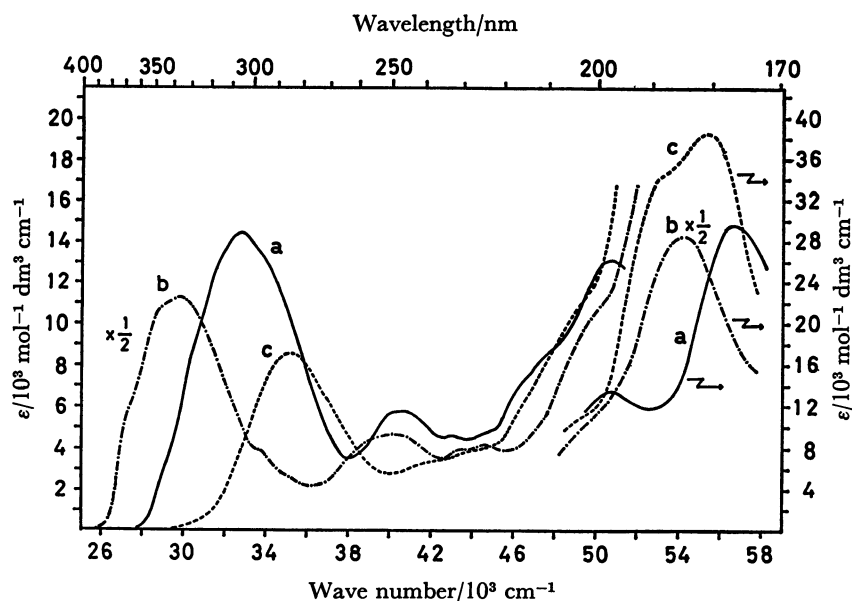


Fig. 2. Near and vacuum UV absorption spectra measured with the heptane solution of (a) BA, (b) DBM, and (c) PPD at room temperature. Absorption intensity of DBM is plotted as one half of the observed one.

TABLE 1. TRANSITION ENERGIES (${}^1\Delta E$ (eV or cm^{-1})) AND OSCILLATOR STRENGTHS (f) OBSERVED AND CALCULATED FOR BENZOYLACETONE (BA)

In heptane			In acetonitrile	In ethanol	Calcd			Assignment
$\frac{{}^1\Delta E}{\text{cm}^{-1}}$	$\frac{{}^1\Delta E}{\text{eV}}$	$f^{\text{a)}$	$\frac{{}^1\Delta E}{\text{eV}}$	$\frac{{}^1\Delta E}{\text{eV}}$	$\frac{{}^1\Delta E}{\text{eV}}$	f	Main config. ^{b)}	
32700	4.06	0.38	4.04	4.03	4.52	0.877	ϕ_1	LE
					4.80	0.017	B_{2u}	LE
40500	5.02	0.10	5.04	5.01	5.60	0.094	$15\leftarrow 2 + \phi_1 + B_{1u}$	LE+CT
43000	5.33	0.06	5.37	5.37	6.02	0.152	$15\leftarrow 3$	CT
44500	5.52		5.56	5.56				
46100 ^{c)}	5.71	0.11	5.71	5.71	6.60	0.242	B_{1u}	LE
47400 ^{c)}	5.88				7.00	0.080	$14\rightarrow 5 + \phi_2$	LE(+BCT)
50800	6.29	0.24	6.28	6.23	7.18	0.233	$14\rightarrow 4$	BCT
56500	7.00	0.63			7.55	0.536	$E_{1u} + E'_{1u}$	LE
					7.60	0.495	$E'_{1u} + E_{1u}$	LE
					8.00	0.626	ϕ_2	LE

a) Oscillator strength was estimated by resolving the spectrum into overlapped bands tentatively. b) Main configurations of respective excited states are shown. In the i - j CT or BCT configuration, i denotes the vacant (*i.e.*, 15th and 16th) or occupied (14th) π -MO's of MA (corresponding to the enol ring), respectively, and j denotes the occupied (2nd and 3rd) or vacant (4th and 5th) π -MO's of the benzene ring, respectively. c) Shoulder.

TABLE 2. TRANSITION ENERGIES (${}^1\Delta E$ (eV or cm^{-1})) AND OSCILLATOR STRENGTHS (f) OBSERVED AND CALCULATED FOR DIBENZOYLMETHANE (DBM)

In heptane			In acetonitrile	In ethanol	Calcd			Assignment ^{c)}
$\frac{{}^1\Delta E}{\text{cm}^{-1}}$	$\frac{{}^1\Delta E}{\text{eV}}$	$f^{\text{a)}$	$\frac{{}^1\Delta E}{\text{eV}}$	$\frac{{}^1\Delta E}{\text{eV}}$	$\frac{{}^1\Delta E}{\text{eV}}$	f	Main config. ^{b)}	
29800	3.69	0.51	3.64	3.63	4.88	1.193	ϕ_1	LE
33800 ^{d)}	4.19	0.05	4.17	4.19	5.09	0.026	B_{2u}	LE _I
(35200) ^{d)}	(4.36)				5.15	0.012	B_{2u}	LE _{II}
40000	4.96	0.23	4.96	4.93	5.66	0.300	$15\leftarrow 2 + B_{1u}$	CT _{II}
					5.92	0.152	$15\leftarrow 2 + \phi_1 + B_{1u}$	LE _I + CT _I
43300	5.37	0.08	5.37	5.37	6.31	0.152	$15\leftarrow 3$	CT _I
44600	5.53		5.51	5.52	6.38	0.151	$15\leftarrow 3$	CT _{II}
46500 ^{d)}	5.76	0.06	6.14	6.05	6.85	0.248	B_{1u}	LE _{II} + LE _I
					6.94	0.172	B_{1u}	LE _I + LE _{II}
49000 ^{d)}	6.08	0.23			7.17	0.253	$14\rightarrow 5 + \phi_2$	BCT _{II} + BCT _I
54100	6.71	1.38	6.65		7.58	0.958	$E'_{1u} + E_{1u} + 14\rightarrow 4$	LE _I + LE _{II}
					7.62	0.462	$E_{1u} + E'_{1u}$	LE _{II}
					7.70	0.689	E'_{1u}	LE _{II}
					7.84	0.589	E_{1u}	LE _I
					8.04	0.420	$14\rightarrow 4$	BCT _I
					8.11	0.004	$14\rightarrow 4$	BCT _{II}

a) See footnote (a) in Table 1. b) See footnote (b) in Table 1. c) LE, CT, or BCT configuration I and II are related to the benzene ring I and II, respectively. d) Shoulder.

molecular geometries predicted by several investigations;^{24-26,41,42)} the results showed that the electronic structure of MA is sensitive to the change of molecular geometry, especially to the position of intramolecularly H-bonded O and H atoms. From the comparison with the observed spectra²⁸⁾ and by referring to the experimental results of microwave spectrum²⁶⁾ and of X-ray crystal analysis of DBM,⁴¹⁾ we have chosen the non-linear asymmetrical H-bond with $R(\text{O}\cdots\text{O})=2.55$ Å and $r(\text{O}-\text{H})=1.18$ Å as one of the plausible structure of MA.

The electronic structure of MA calculated by the modified CNDO-CI method is tabulated in Table 4, together with the observed values.²⁸⁾ The agreement between the theoretical and observed values is satisfactory for the lower excited states. It is noteworthy that the first and the second σ - σ^* bands predicted at 8.76 and 9.35 eV, respectively, is the CT band pertinent to the H-bond in the sense that the CT configurations, 13—17 and 13—18 in the H-bond (corresponding to the transition from $\text{O}-\text{H}\cdots\text{O}$ structure to $\text{O}\cdots\text{H}-\text{O}$ structure in the valence-bond scheme²⁹⁾) mainly contribute

TABLE 3. TRANSITION ENERGIES (${}^1\Delta E$ (eV or cm^{-1})) AND OSCILLATOR STRENGTHS (f) OBSERVED AND CALCULATED FOR 3-PHENYL-2,4-PENTANEDIONE (PPD)

In heptane			In acetonitrile	In ethanol	Calcd			Assignment
$\frac{{}^1\Delta E}{\text{cm}^{-1}}$	$\frac{{}^1\Delta E}{\text{eV}}$	f^a	$\frac{{}^1\Delta E}{\text{eV}}$	$\frac{{}^1\Delta E}{\text{eV}}$	$\frac{{}^1\Delta E}{\text{eV}}$	f	Main config. ^{b)}	
35200	4.37	0.19	4.34	4.33	4.48	0.314	ϕ_1	LE
					4.86	0	B_{2u}	LE
41500	5.14	0.04	5.12	5.12	5.29	0.040	$15 \leftarrow 2$	CT
43800	5.43	0.04	5.39	5.39	5.45	0.002	$15 \leftarrow 3$	CT
46900 ^{c)}	5.82	0.06			5.91	0.196	$B_{1u} + 14 \rightarrow 5$	LE
49000 ^{c)}	6.08	0.10	6.05	6.05	6.31	0.280	$B_{1u} + 14 \rightarrow 5$	LE
52500	6.51	0.39	6.63		6.54	0.143	$14 \rightarrow 4$	BCT
					6.68	0.643	$\phi_2 + E_{1u} + 14 \rightarrow 5$	LE
55400	6.87	0.70			7.06	0.996	E'_{1u}	LE
					7.37	0.203	$16 \leftarrow 2 + E_{1u}$	CT+LE
					7.55	0.043	$\phi_2 + 16 \leftarrow 2$	LE

a) See footnote (a) in Table 1. b) See footnote (b) in Table 1. c) Shoulder.

TABLE 4. SINGLET AND TRIPLET TRANSITION ENERGIES (${}^1\Delta E$ AND ${}^3\Delta E$ (eV)) AND OSCILLATOR STRENGTHS (f) OBSERVED AND CALCULATED FOR MALONALDEHYDE (MA)

Assignment	Obsd ^{a)}		Calcd			Main config. ^{c)}
	${}^1\Delta E$	f	${}^1\Delta E$	${}^3\Delta E$	f^b	
$n-\pi^*$	3.51			3.33	0.000 (z)	13—15
$\pi-\pi^*$	4.71 (5.08) ^{d)}	0.3	5.18	3.92	0.114 (x)	14—15
$n-\pi^*$				6.29	0.000 ₃ (z)	13—16
$\pi-\sigma^*$				7.44	0.008 (z)	14—17
$\sigma-\pi^*$				7.51	0.003 (z)	12—15
$\pi-\pi^*$	>6.3	>0.2	7.87	5.85	0.239 (y)	14—16
$\pi-\sigma^*$				8.18	0.019 (z)	14—18
$\sigma-\pi^*$				8.72	0.015 (z)	12—16, 9—15
$\sigma(n)-\sigma^*$			8.76	8.40	0.012 (\overline{xy}) ^{e)}	13—18, 13—17, 13—19
$\pi-\sigma^*$				9.15	0.026 (z)	14—19
$\sigma(n)-\sigma^*$			9.35	7.35	0.372 (x)	13—17, 13—18
$\sigma-\sigma^*$			9.46	9.25	0.014 (\overline{xy}) ^{e)}	13—19, 13—18
$\pi-\pi^*$			9.81	8.44	0.203 (\overline{xy}) ^{e)}	11—15
$\pi-\sigma^*$				9.83	0.019 (z)	14—20
$\sigma-\pi^*$				10.40	0.000 ₃ (z)	10—15
$\pi-\sigma^*$				11.03	0.003 (z)	14—21, 14—22, 11—19
$\sigma-\sigma^*$			11.03	10.74	0.058 (x)	13—20
$\sigma-\pi^*$				11.04	0.002 (z)	7—15

a) Observed value in the vapor phase taken from Ref. 28. b) Oscillator strength is calculated for the singlet manifold. The direction of transition moment is shown in parentheses, x-, y-, and z-axes being taken as in Fig. 1. c) Singly excited configuration, $i-j$, denotes one-electron excitation from the i -th occupied MO to the j -th vacant MO. The 14th MO is the highest occupied one. d) Observed value in ethanol. e) x- and y-components of transition moment contribute equally with opposite signs.

to the first (55.8%) and to the second (53.5%) $\sigma-\sigma^*$ excited states. The CT configurations also contribute considerably (11.6%) to the first $\pi-\pi^*$ excited state of MA as in the case of the corresponding band of the enol form of acac and its fluoro derivatives.^{29,30)}

Electronic Structures of BA, DBM, and PPD. The electronic structures of the π -electron systems of BA, DBM, and PPD were calculated by the method of composite molecule^{31,32)} in which the β -diketone is divided into the enol ring and the benzene ring(s). The rotating angle, θ , between the enol ring and the

benzene ring (Fig. 1) was treated as a variable. Figure 3 shows the θ -dependence of energy levels calculated for BA, DBM, and PPD.⁴³⁾ By referring to the absorption spectra in Fig. 2, and also by referring to the observed θ -value of DBM (16.9°)⁴¹⁾ and tetraacetyl-ethane (89°)⁴²⁾ in crystalline state, theoretical results with $\theta=20^\circ$ are taken to BA and DBM, and the result with $\theta=70^\circ$, to PPD, as tabulated in Tables 1—3. The theoretical energy diagrams of BA and DBM are illustrated in Fig. 4 and the one of PPD, in Fig. 5.

As is shown in Table 1 and in Fig. 4, the first allowed

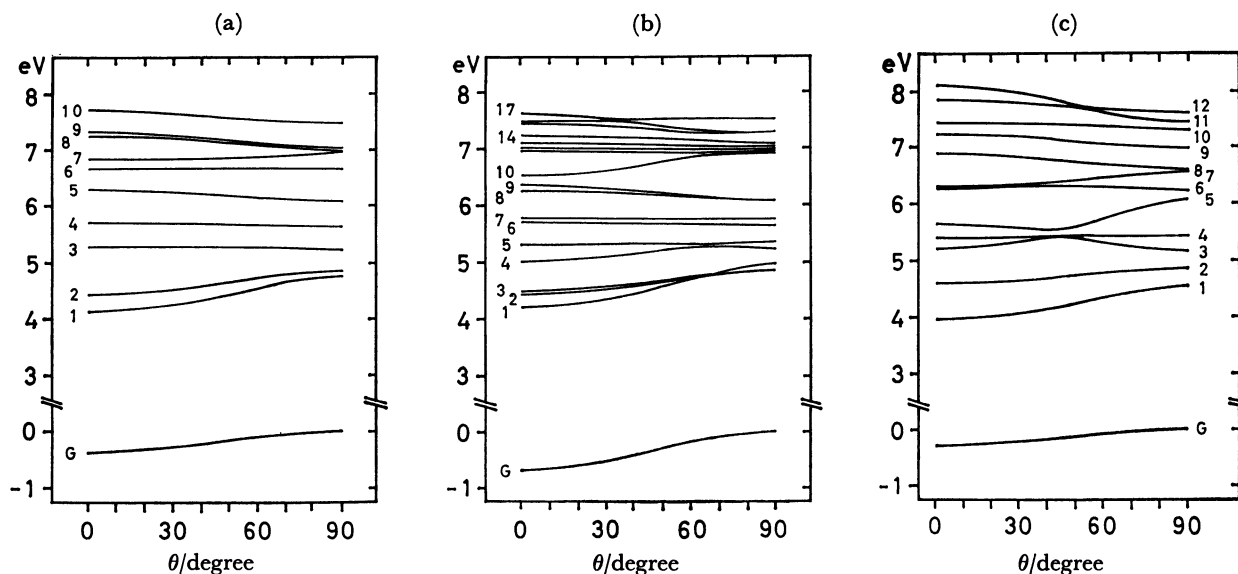


Fig. 3. θ -dependence of energy levels calculated for (a) BA, (b) DBM, and (c) PPD.

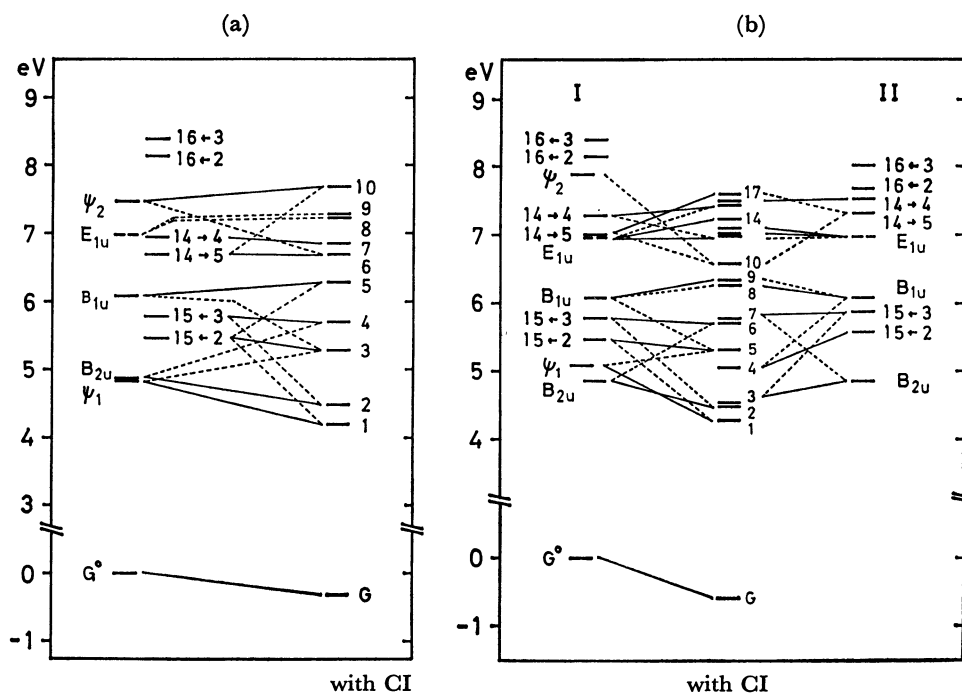


Fig. 4. Energy levels calculated with and without CI treatment for (a) BA and (b) DBM. In DBM, the configurations related to the benzene ring I and the LE configurations of the enol ring are shown on the left column and the configurations related to the benzene ring II, on the right column. For the CT or BCT configuration, $i-j$, see the footnote (b) in Table 1.

band of BA observed at 32700 cm^{-1} in heptane can safely be assigned to the LE state of the enol ring, ψ_1 (60.3%) mixed with the CT (from the benzene ring to the enol ring) (18.5%) and BCT (from the enol ring to the benzene ring) (9.6%) configurations. The second excited state of BA which is mainly (73.2%) composed of B_{2u} state of the benzene ring and the absorption intensity of which is predicted to be weak may be covered with the first $\pi-\pi^*$ band. The assignment may be supported from the fact that the corre-

sponding band of DBM is observed near 33800 cm^{-1} as a shoulder. The 40500 cm^{-1} band of BA can be assigned to the third excited state which is mainly composed of the $15\leftarrow 2$ CT (42.4%), and ψ_1 (26.7%) and B_{1u} (19.6%) LE configurations. The 44000 cm^{-1} band has two peaks at 43000 and 44500 cm^{-1} in heptane and can be assigned to the fourth excited state which is mainly composed of the $15\leftarrow 3$ CT (55.8%) and B_{2u} LE (22.7%) configurations. The 44000 cm^{-1} band is the CT band between the benzene and enol rings.

From the comparison with the theoretical result, we can expect three bands in the 45000–53000 cm^{-1} region. The shoulder at $\approx 46100 \text{ cm}^{-1}$ is assigned to the fifth excited state which is mainly composed of the B_{1u} LE (61.8%) and $15 \leftarrow 2$ CT (20.1%) configurations. To the 6th and 7th excited states, BCT configurations contribute significantly. The 6th excited state is mainly composed of the $14 \rightarrow 5$ BCT (41.9%), and ϕ_2 (24.1%), ϕ_1 (9.4%), E_{1u} (11.1%), and B_{1u} (9.2%) LE configurations, and is tentatively assigned to the weak shoulder near 47400 cm^{-1} . The 7th excited state which is safely assigned to the 50800 cm^{-1} band is the BCT band to which the $14 \rightarrow 4$ BCT (64.8%) and E'_{1u} LE (19.4%) configurations mainly contribute.

The very strong 56500 cm^{-1} band is predicted to be composed of three bands, *i.e.*, 8th–10th excited states. The 8th and 9th excited states are mainly composed of the E_{1u} and E'_{1u} LE configurations (47.4% and 18.6%, respectively, for the 8th, and 26.2% and 31.6%, respectively, for the 9th excited state) mixed with BCT and CT configurations. The 10th excited state is mainly composed of the ϕ_2 LE (51.9%) and $14 \rightarrow 5$ BCT (20.8%) configurations.

The electronic structure of DBM is illustrated in Fig. 4, compared with the one of BA. Because two benzene rings, I and II interact with the enol ring, the 2nd and 3rd, 4th and 5th, 6th and 7th, and 8th and 9th excited states of DBM appear in pairs with the corresponding character related to each benzene ring. As is shown in Table 2, the observed bands at 29800, 33800, 40000, and 44000 cm^{-1} in heptane can be assigned to the first, 2nd and 3rd, 4th and 5th, and 6th and 7th excited states, respectively. The character of the bands is semiquantitatively the same to the corresponding first four bands of BA. The 44000 cm^{-1} band has two peaks at 43300 and 44600 cm^{-1} as in the case of BA. In the 46000–50500 cm^{-1} region, three bands, *i.e.*, 8th–10th excited states are predicted to overlap. The character of the pair (*i.e.*, the 8th and 9th) and the 10th excited states corresponds to the one of the 5th and 6th excited states of BA, respectively. In the very strong 54100 cm^{-1} region, six bands corresponding to the 11th–16th excited states are expected to locate. The 11th–14th states are mainly composed of the E_{1u} and E'_{1u} LE configurations of two benzene rings, and the 15th and 16th excited states, of the $14 \rightarrow 4$ BCT configuration from the enol ring to each benzene ring.

In conclusion, theoretical investigation of the spectra clearly shows strong π -electron interaction between the enol and benzene rings in BA and DBM.

Contrary to BA and DBM, the spectrum of PPD is well reproduced when θ value around 70° is employed, indicating that π -electron interaction between the enol and benzene rings is weak. The theoretical result of PPD with $\theta = 70^\circ$ is shown in Table 3 and in Fig. 5. Because the PPD molecule is of approximate C_2 symmetry and because the π -electron interaction between the rings is rather weak, configuration interaction in PPD is more limited than in BA. As is shown in Table 3, qualitative assignment for each band is similar to the one of BA. The 35200 cm^{-1} band assigned to the first excited state is the LE state, ϕ_1 (87.3%), and the

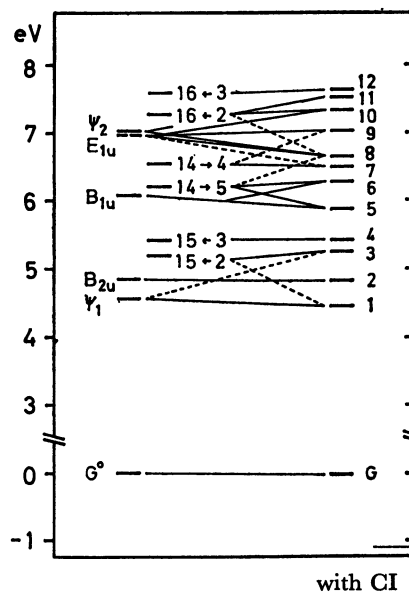


Fig. 5. Energy levels calculated with and without CI treatment for PPD. For the CT or BCT configuration, $i-j$, see the footnote (b) in Table 1.

second excited state is B_{2u} state of the benzene ring (97.4%). The latter band is again too weak to be observed. The 41500 cm^{-1} band assigned to the third excited state is the $15 \leftarrow 2$ CT state (86.3%), and the 43800 cm^{-1} band assigned to the 4th excited state is the $15 \leftarrow 3$ CT state (97.8%).

The B_{1u} LE and $14 \rightarrow 5$ BCT configurations contribute predominantly to the 5th (50.9% and 34.7%, respectively) and to the 6th (47.1% and 39.3%, respectively) excited states, which are tentatively assigned to the shoulders at 46900 cm^{-1} and 49000 cm^{-1} , respectively. To the strong 52500 cm^{-1} region, the 7th ($14 \rightarrow 4$ BCT (85.8%)) and the 8th (ϕ_2 (32.4%) + E_{1u} (32.1%) + $14 \rightarrow 5$ BCT (24.7%)) excited states can be assigned. To the very strong 55400 cm^{-1} region, the strong 9th (E'_{1u} (82.6%)) and 10th (E_{1u} (39.4%) + $16 \leftarrow 2$ CT (51.3%)) excited states mainly contribute.

Theoretical oscillator strength of the first band predicts well the increase of the observed transition intensity in the order of $\text{PPD} < \text{BA} < \text{DBM}$. Table 5 shows coefficients of several main configurations in the ground and the first excited states. The wave functions clearly show that the increase of the interaction of the $15 \leftarrow 2$ CT configuration with the ground and ϕ_1 LE configurations is mainly responsible for the increase of the transition intensity.

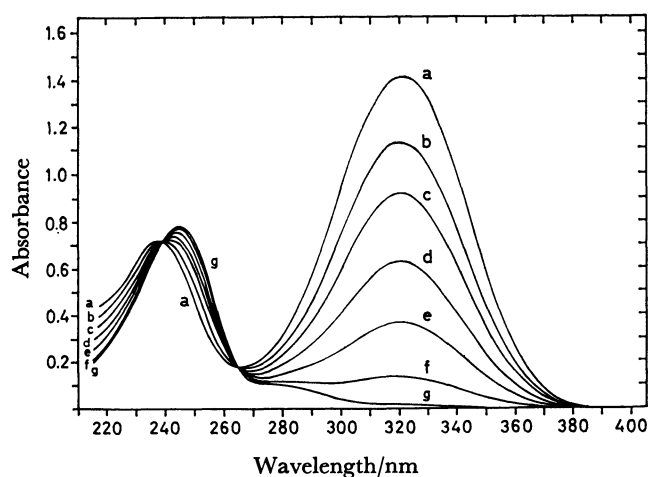
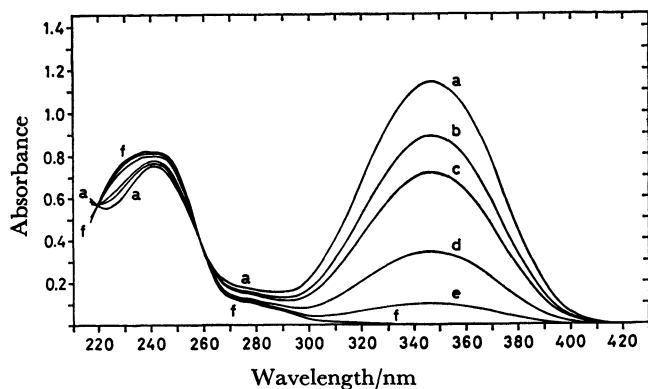
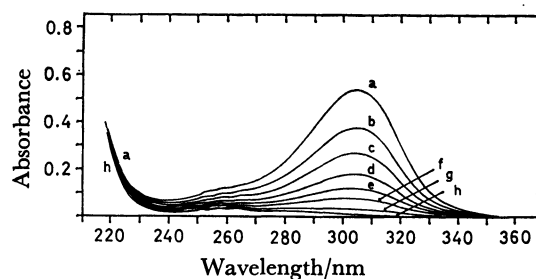
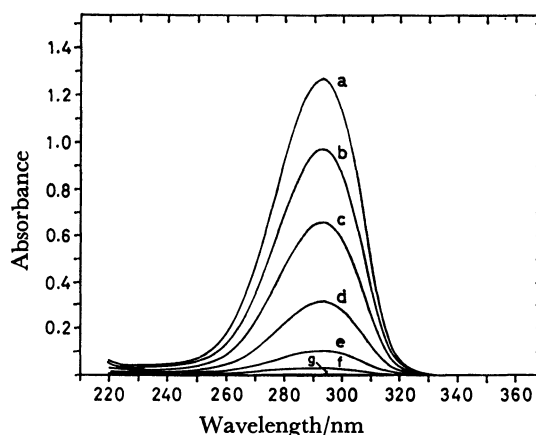
UV Absorption Spectra in KOH Aqueous Solution.

Near UV absorption spectra measured with the KOH aqueous solutions of BA, DBM, PPD, and acac are shown in Fig. 6. The strong bands at 320.5 nm of BA, at 347 nm of DBM, and at 304.5 nm of PPD can be assigned to the first $\pi-\pi^*$ band of the anion with planar chelate ring as in the case of the 292.5 nm band of the acac anion.²⁹ As is shown in Fig. 6, the spectra of the KOH aqueous solutions were found to change with time, and the strong bands at 300–350 nm finally disappear. In Fig. 7, time dependence of the absorbance, $\Delta A (= A(t) - A(t=\infty))$, for the 320.5 nm band of the

TABLE 5. WAVE FUNCTIONS (COEFFICIENTS OF MAIN CONFIGURATIONS) OF THE GROUND AND THE FIRST π - π^* EXCITED STATES OF BA, DBM, AND PPD

Configuration ^{a)}	BA		DBM		PPD	
	Ground state	1st π - π^* state	Ground state	1st π - π^* state	Ground state	1st π - π^* state
G ^o	0.9728	-0.0835	-0.9554	0.0620	0.9973	0.0062
ϕ_1 LE	0.0051	0.7767	-0.0039	-0.7202	-0.0003	0.9341
B _{1u} LE I	-0.0177	-0.2151	0.0159	0.2331	0.0006	0.0488
E _{1u} LE I	0.0157	0.2228	-0.0139	-0.2333	-0.0005	-0.0705
II			-0.0130	0.1115		
15 \leftarrow 2 CT I	-0.1909	-0.4134	0.1779	0.4667	0.0241	-0.3370
II			-0.1475	0.1389		
16 \leftarrow 2 CT I	0.1044	0.1194	-0.0983	-0.1362	-0.0385	0.0391
II			-0.1244	0.0600		
14 \rightarrow 5 BCT I	-0.0696	0.3104	0.0631	-0.2589	-0.0571	-0.0629
II			0.0004	0.1292		
f {calcd		0.877		1.193		0.314
{obsd		0.38		0.51		0.19

a) Configuration I or II is related to the benzene ring I or II, respectively.

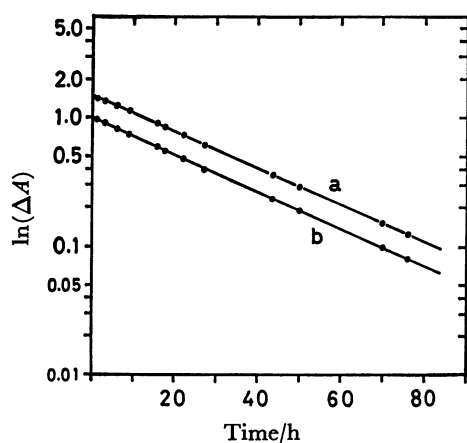
Fig. 6A. Near UV absorption spectra measured with the KOH aqueous solution of BA at (a) $t=0.8$ h, (b) $t=8.7$ h, (c) $t=15.5$ h, (d) $t=27.0$ h, (e) $t=43.4$ h, (f) $t=75.9$ h, and (g) $t=163.8$ h.Fig. 6B. Near UV absorption spectra measured with the KOH aqueous solution of DBM at (a) $t=1.0$ h, (b) $t=6.1$ h, (c) $t=10.1$ h, (d) $t=25.0$ h, (e) $t=50.8$ h, and (f) $t=151.4$ h.Fig. 6C. Near UV absorption spectra measured with the KOH aqueous solution of PPD at (a) $t=24$ min, (b) $t=29$ min, (c) $t=35$ min, (d) $t=42$ min, (e) $t=49$ min, (f) $t=57$ min, (g) $t=76$ min, and (h) $t=194$ min.Fig. 6D. Near UV absorption spectra measured with the KOH aqueous solution of acac at (a) $t=0.8$ h, (b) $t=9.1$ h, (c) $t=22.3$ h, (d) $t=49.6$ h, (e) $t=94.6$ h, (f) $t=145.0$ h, and (g) $t=239.2$ h.

BA anion is shown as an example; the absorbance (ΔA) decreases exponentially with time. The exponential decay of the absorbance was also observed for the first π - π^* bands of the DBM, PPD, and acac

TABLE 6. RATE CONSTANT (k (s⁻¹)), INITIAL ABSORBANCE (ΔA_0), AND INITIAL MOLAR EXTINCTION COEFFICIENT^{a)} (ϵ_0) FOR THE FIRST BAND OF THE KOH AQUEOUS SOLUTION OF BA, DBM, PPD, AND acac

	BA		DBM		PPD			acac	
$[\beta\text{-diketone}] \times 10^4/\text{M}$	8.53	7.78	6.21	5.76	19.55	12.03	14.50	4.2	5.76
$[\text{KOH}] \times 10/\text{M}$	9.52	0.894	9.52	0.894	0.248	0.119	0.0594	9.52	0.991
$k \times 10^5/\text{s}^{-1}$	10.2	0.904	14.3	1.39	116	102	113	13.8	0.846
ΔA_0	1.67	1.49	1.35	1.20	3.65	2.23	2.70	1.01	1.29
ϵ_0	18700	18300	20700	19800	17800	17700	17700	23000	21300
Average	18500		20300		17700			22200	

a) Estimated at the band maximum.

Fig. 7. Time dependence of the absorption intensity (ΔA) measured with the first π - π^* band of the BA anion at (a) 320.5 nm and (b) 340 nm.

anions, indicating that the spectral change is due to the unimolecular reaction, $A \rightarrow A'$, of the anions. The rate constants (k) under several experimental conditions are listed in Table 6. In the BA, DBM, and acac anions, the rate constant is roughly proportional to the concentration of KOH, strongly suggesting that the planar structure of the chelate ring is broken by the action of the KOH molecules. Under the fixed concentration of KOH, the rate constant increases in the order of the $\text{BA} < \text{acac} < \text{DBM} \ll \text{PPD}$ anions. The true absorption intensity of the 300–350 nm band of the anion can be evaluated from the extrapolated absorbance at $t=0$ (ΔA_0) with the correction of the final absorbance ($A(t=\infty)$). The results are tabulated in Table 6. The absorption intensities are rather equal for the PPD, BA, and DBM anions in contrast to the ones of the corresponding bands in neutral species.

The authors wish to express their sincere thanks to Professor Saburo Nagakura, the University of Tokyo, for valuable discussions and for reading manuscript carefully.

References

- 1) O. Dimroth, *Ann.*, **399**, 91 (1913).
- 2) E. M. Kosower, *J. Am. Chem. Soc.*, **80**, 3267 (1958).
- 3) R. S. Rasmussen, D. D. Tunnicliff, and R. R. Brattain, *J. Am. Chem. Soc.*, **71**, 1068 (1949).
- 4) S. Bratož, D. Hadži, and G. Rossmy, *Trans. Faraday Soc.*, **52**, 464 (1956).
- 5) K. L. Wierzchowski and D. Shugar, *Spectrochim. Acta*, **21**, 943 (1965).
- 6) J. U. Lowe, Jr., and L. N. Ferguson, *J. Org. Chem.*, **30**, 3000 (1965).
- 7) H. Ogoshi and K. Nakamoto, *J. Chem. Phys.*, **45**, 3113 (1966).
- 8) H. Ogoshi and Z. Yoshida, *Spectrochim. Acta, Part A*, **27**, 165 (1971).
- 9) E. Grens, A. Grinvalde, and J. Stradinš, *Spectrochim. Acta, Part A*, **31**, 555 (1975).
- 10) J. L. Burdett and M. T. Rogers, *J. Am. Chem. Soc.*, **86**, 2105 (1964); M. T. Rogers and J. L. Burdett, *Can. J. Chem.*, **43**, 1516 (1965).
- 11) R. L. Lintvedt and H. F. Holtzclaw, Jr., *J. Am. Chem. Soc.*, **88**, 2713 (1966); *Inorg. Chem.*, **5**, 239 (1966).
- 12) M. Tanaka, T. Shono, and K. Shinra, *Bull. Chem. Soc. Jpn.*, **42**, 3190 (1969).
- 13) R. H. Holm and F. A. Cotton, *J. Am. Chem. Soc.*, **80**, 5658 (1958).
- 14) M. Mikami, I. Nakagawa, and T. Shimanouchi, *Spectrochim. Acta, Part A*, **23**, 1037 (1967).
- 15) G. T. Behnke and K. Nakamoto, *Inorg. Chem.*, **6**, 433, 440 (1967).
- 16) R. A. Morton, A. Hassan, and T. C. Calloway, *J. Chem. Soc.*, **1934**, 883.
- 17) L. Sacconi and G. Giannoni, *J. Chem. Soc.*, **1954**, 2751.
- 18) G. S. Hammond, W. G. Borduin, and G. A. Guter, *J. Am. Chem. Soc.*, **81**, 4682 (1959).
- 19) Y. Murakami and K. Nakamura, *Bull. Chem. Soc. Jpn.*, **39**, 901 (1966).
- 20) P. Gacoin, *J. Chem. Phys.*, **57**, 1418 (1972).
- 21) D. W. Barnum, *J. Inorg. Nucl. Chem.*, **21**, 221 (1961); **22**, 183 (1961).
- 22) P. Schuster, *Chem. Phys. Lett.*, **3**, 433 (1969).
- 23) A. D. Issacson and K. Morokuma, *J. Am. Chem. Soc.*, **97**, 4453 (1975).
- 24) G. Karlström, B. Jönsson, B. Roos, and H. Wennerström, *J. Am. Chem. Soc.*, **98**, 6851 (1976).
- 25) J. E. Del Bene and W. L. Kochenour, *J. Am. Chem. Soc.*, **98**, 2041 (1976).
- 26) W. F. Rowe, Jr., R. W. Duerst, and E. B. Wilson, *J. Am. Chem. Soc.*, **98**, 4021 (1976).
- 27) J. E. Del Bene, *Chem. Phys. Lett.*, **44**, 512 (1976).
- 28) C. J. Seliskar and R. E. Hoffman, *Chem. Phys. Lett.*, **43**, 481 (1976); *J. Am. Chem. Soc.*, **99**, 7072 (1977).
- 29) H. Nakanishi, H. Morita, and S. Nagakura, *Bull. Chem. Soc. Jpn.*, **50**, 2255 (1977).
- 30) H. Nakanishi, H. Morita, and S. Nagakura, *Bull. Chem. Soc. Jpn.*, **51**, 1723 (1978).
- 31) H. C. Longuet-Higgins and J. N. Murrell, *Proc. Phys.*

- Soc. (London)*, **A68**, 601 (1955); J. N. Murrell, *ibid.*, **A68**, 969 (1955).
- 32) K. Kimura and S. Nagakura, *Mol. Phys.*, **9**, 117 (1965).
- 33) K. Kaya and S. Nagakura, *J. Mol. Spectrosc.*, **44**, 279 (1972).
- 34) H. Morita, K. Fuke, and S. Nagakura, *Bull. Chem. Soc. Jpn.*, **50**, 645 (1977).
- 35) Re-measured in the present study.
- 36) D. W. Turner, C. Baker, A. D. Baker, and C. R. Brundle, "Molecular Photoelectron Spectroscopy," John Wiley, London (1970).
- 37) S. Evans, A. Hamnett, A. F. Orchard, and D. R. Lloyd, *Faraday Discuss. Chem. Soc.*, **54**, 227 (1972).
- 38) C. Nishijima, H. Nakayama, T. Kobayashi, and K. Yokota, *Chem. Lett.*, **1975**, 5.
- 39) G. Klopman, *J. Am. Chem. Soc.*, **86**, 4550 (1964); **87**, 3300 (1965).
- 40) J. A. Pople, *Proc. Phys. Soc.*, **A68**, 81 (1955).
- 41) D. E. Williams, *Acta Crystallogr.*, **21**, 340 (1966).
- 42) J. P. Schaefer and P. J. Wheatley, *J. Chem. Soc., A*, **1966**, 528.
- 43) When $\theta \neq 0^\circ$, the CT configurations can interact with low-lying $n-\pi^*$ LE configurations in the enol ring through the resonance integral, $\beta_{n\pi}$, between the n -orbital in the enol ring and the occupied π -MO in the benzene ring. Because the $\beta_{n\pi}$ value is very small even when θ is large, the influence of the $n-\pi^*$ LE configurations on the π -electronic structure is negligibly small.
-